Designed Variants of Recombinant ACE2-Fc that Decouple Anti-SARS-CoV-2 Activities from Unwanted Cardiovascular Effects

Pan Liu[1], Xinfang Xie[1], Li Gao[1], and Jing Jin[1]*

[1]Feinberg Cardiovascular and Renal Research Institute, Department of Medicine-Nephrology and Hypertension, Northwestern University Feinberg School of Medicine, Chicago, IL

[2]Department of Nephrology, The First Affiliated Hospital of Medical College, Xi'an Jiaotong University, Xi'an, China

*Correspondence to: Jing Jin, 303 E. Superior Street, Room 8-518, Chicago, IL 60611, Tel. 312-503-8190, Email: jing.jin@northwestern.edu

Abstract

Angiotensin-converting enzyme 2 (ACE2) is the entry receptor for SARS-CoV-2, and recombinant ACE2 decoys are being evaluated as new antiviral therapies. We designed and tested an ACE2-Fc fusion protein, which has the benefits of a long pharmacological half-life and the potential to facilitate immune clearance of the virus. Out of the concern that the intrinsic catalytic activity of ACE2 may unintentionally alter the balance of its hormonal substrates and cause adverse cardiovascular effects in treatment, we performed a mutagenesis screening for inactivating the enzyme. Three mutants, R273A, H378A and E402A, completely lost their enzymatic activity for either surrogate or physiological substrates. All of them remained capable of binding SARS-CoV-2 and could suppress the transduction of a pseudotyped virus in cell culture. This study established new ACE2-Fc candidates as antiviral treatment for SARS-CoV-2 without potentially harmful side effects from ACE2's catalytic actions toward its vasoactive substrates.

Introduction

As COVID-19 pandemic is still unfolding and no specific antiviral treatments are available, there is an unmet need to explore new drug candidates that are effective and safe, and broad spectrum against the evolving virus. In addition to the ongoing clinical trials of repurposed compounds and patient-derived antibodies, new drugs are being developed through targeted screening and rational design.

One of the focuses is on drug candidates that target receptor-mediated viral entry. A diverse group of human coronaviruses including SARS-CoV of 2002, HCoV-NL63 of 2004 and SARS-CoV-2 of COVID-19 rely on their spike proteins to bind ACE2 cell receptor as the first step in viral entry(Hoffmann et al., 2020; Wrapp et al., 2020; Yan et al., 2020; P. Zhou et al., 2020). It has been shown that soluble ACE2 at generous abundance as compared to viral concentration can lower infectivity of cultured human cells, similar to experimental anti-spike antibodies(Iwanaga et al., 2020; Lei et al., 2020; Monteil et al., 2020). Prior to the pandemic, one of the human recombinant soluble ACE2 (hrsACE2) drugs developed by Apeiron Biologics and GlaxoSmithKline (GSK) had completed Phase I and Phase II clinical trials for human pulmonary arterial hypertension and acute respiratory distress syndrome (ARDS) (Hemnes et al., 2018; Khan et al., 2017), and is now repositioned for investigational treatment of COVID-19 (ClinicalTrials.gov identifier: NCT04335136).

The current focus has been on improving binding affinity, pharmacokinetic/pharmacodynamic (PK/PD), antiviral specificity and neutralization efficacy of ACE2-based biologics through bioengineering design(Chan et al., 2020; Kruse, 2020; Lei et al., 2020). Also in a different context unrelated to COVID-19, our group had

46 previously constructed a chimeric fusion between the ectodomain of ACE2 and the Fc segment of IgG1
47 ("hinge" plus CH2 and CH3 regions) (**Fig1A**). In keeping with a well-recognized function of Fc to extend
48 protein half-life through its cognate neonatal Fc receptor (FcRn), ACE2-Fc outlasted untagged soluble ACE2
49 by ~100 folds in mice(Liu et al., 2018). The enzymatic activity of ACE2 in the fusion degraded angiotensin II
50 (AngII) and rendered blood pressure control for up to two weeks. In comparison to its untagged counterpart,
51 ACE2-Fc is predicted to offer superior pharmacological benefits(Kruse, 2020), which make it also suitable for
52 prophylactic usages by frontline healthcare workers in hospital and caregivers of COVID-19 patients at
53 home(Kruse, 2020).

54 Our study also attempts to address another potential drawback of the original hrsACE2 biologic. Although
55 it was initially believed that the catalytic activity of ACE delivered in an excess quantity through therapeutic
56 hrsACE2 acting on RAAS may alleviate ARDS in severe COVID-19 cases(Imai et al., 2005; Khan et al., 2017),
57 the relevance in human disease remains controversial(Cai et al., 2020; Guzik et al., 2020; Lumbers, Delforce,
58 Pringle, & Smith, 2020; Rossi, Sanga, & Barton, 2020). COVID-19 mortality is prevalent among patients with
59 underlying conditions such as cardiovascular disease (32%), diabetes (30%) and chronic lung disease (18%)
60 (CDC data), a large number of COVID-19 patients are on existing ACEI/ARB blockade therapy for preexisting
61 cardiovascular diseases and certain diabetic complications(Zheng, Ma, Zhang, & Xie, 2020). There have been
62 conflicting results on whether RAAS blockade medications had improved or worsened COVID-19
63 recovery(Bavishi, Maddox, & Messerli, 2020; Danser, Epstein, & Batlle, 2020; South, Brady, & Flynn, 2020;
64 Sparks et al., 2020; Vaduganathan et al., 2020). However, studies discovered a correlation between RAAS
65 blockade and upregulation of endogenous ACE2 expression(Guo, Huang, Lin, & Lv, 2020; Mehra, Desai, Kuy,
66 Henry, & Patel, 2020; Sommerstein, Kochen, Messerli, & Grani, 2020; South, Diz, & Chappell, 2020; F. Zhou
67 et al., 2020), expected to have a potential harmful effect. The carboxypeptidase activity of ACE2 hydrolyses a
68 broad range of vasoactive hormonal substrates including AngII, apelin-13, bradykinin, among others, and
69 exerts complex changes of blood pressure and fluid balance through coordinated actions of the heart, the
70 blood vessels, the kidney and the lung. Severe cases of SARS-CoV-2 infection frequently have multiorgan
71 involvement(Bosmuller et al., 2020; Menter et al., 2020; Noris, Benigni, & Remuzzi, 2020; Renu, Prasanna, &
72 Valsala Gopalakrishnan, 2020; Zaim, Chong, Sankaranarayanan, & Harky, 2020) that adds difficulty to
73 treatments. In addition, there are concerns that RAAS antagonist medications could be associated with
74 pulmonary adverse drug events in COVID-19 morbidity and mortality(Stafford et al., 2020). In our view, the
75 dual function of investigational drug hrsACE2 to simultaneously act on viral neutralization and RAAS can
76 potentially complicate clinical assessment of therapeutic efficacy. In order to achieve an exclusive antiviral

77 function in an ACE2-derived biologic, we sought to modify ACE2 catalytic center to limit the catalysis of its
78 vasoactive substrates.

79 **Results**

80 **ACE2-Fc mutagenesis strategy to remove catalytic activity**

81 We constructed an ACE2-Fc template by using the ectodomain of ACE2 fused with an Fc sequence
82 (**Fig1A**). The chimeric fusion naturally formed a dimer of >250 kDa as expected (**Fig1B**). There is an extensive
83 amount of information with regard to the structural characteristics of ACE2 in relationship to SARS-CoV-2
84 receptor-binding domain (RBD)(Lan et al., 2020; Shang et al., 2020; Walls et al., 2020; Wang et al., 2020;
85 Wrapp et al., 2020; Yan et al., 2020). SARS-CoV-2 binds a surface segment of ACE2 through the apex of its
86 spike protein (**Fig1C**). ACE2 is a metallopeptidase that requires divalent cation such as zinc for activity. A Zn^{2+}
87 ion is buried deep in the catalytic cleft within the proximal lobe relative to the viral binding site. Based on an
88 inhibitor-bound structure of ACE2(Towler et al., 2004), both proximal and distal residues that line the
89 catalytic cleft form interactions with the inhibitor, which occupies the presumed substrate pocket (**Fig1D**).
90 Zn^{2+} is coordinated by three residues, His374, His378 and Glu402, which are the obvious choices for
91 mutagenesis when making enzymatically inactive mutants(Lei et al., 2020) (**Fig1E**). In addition to these Zn^{2+}-
92 binding sites, we sought to look for catalytic residues in contact with the substrates that are further away
93 from RBD binding segment. The inhibitor-bound structure indicates six residues that extend their side chains
94 toward the substrate direction. These are Glu145, Arg273, Pro346, His345, Asp368 and His505 (**Fig1F**).

95 **Substrate-dependent inactivation among ACE2-Fc mutants**

96 Next, we made alanine-substitution of each residue including the three that bind Zn^{2+} and the additional
97 six that potentially bind substrates (supplementary figure S1). Wild-type and 9 mutants of ACE2-Fc were
98 produced using a HEK293 expression system as soluble proteins (**Fig1B**). Purified proteins were subjected to
99 a set of enzymatic assays using a surrogate Mca-APK(Dnp) fluorogenic substrate and physiological substrates
100 such as AngII and apelin-13 (**Fig2**). It should be noted that although the surrogate substrate Mca-APK(Dnp) is
101 traditionally used for measuring ACE2 activity, the sequence does not resemble those of the physiological
102 substrates, which share a Pro-Phe motif at their C-termini (Supplementary figure S2). Instead, the catalysis
103 of AngII and apelin-13 by ACE2-Fc variants was measured by the hydrolysis rate of their C-terminus Phe
104 amino acid(Liu et al., 2017).

105 We performed Mca-APK(Dnp) measurements, alongside phenylalanine hydrolysis assays using AngII and
106 apelin-13 as substrates to determine the enzymatic activities of the ACE2-Fc variants (**Fig2A-C**). In order to

107 better characterize the catalytic performances of individual ACE2-Fc mutants relative to their wild-type
108 counterpart, we conducted two types of enzymatic assays. The first method used an excess amount of the
109 enzyme (100 ng) in reactions with varying concentrations of the three substrates. This would potentially
110 detect low partial activity of enzymes. The second method had a lower amount of purified ACE2-Fc variants
111 (10 ng each) to react with an excess quantity of the substrates (2 or 10 nmol: see Methods) in order to
112 distinguish among mutants with high activities. As it turned out, the results from these two methods were to
113 an extend in agreement with each other (**Fig2**: left panels compared to right panels). One of the surprising
114 findings was that there was a clear evidence of substrate-dependent inactivation of individual mutations,
115 particularly among those lining the inhibitor/substrate space. For instance, while Mca-APK(Dnp) showed no
116 activity of 7 ACE2-Fc mutants, including 4 substrate-binding residues of Arg273Ala, His345Ala, Pro346Ala
117 and His505Ala (**Fig2A**), His345Ala, Pro346Ala and His505Ala remained active toward AngII and apelin-13
118 (**Fig2B,2C**). In addition, His374Ala, one of the Zn^{2+}-binding residues, retained a low level of activity against
119 Apelin-13 (**Fig2C**). When all three substrates are considered, Arg273Ala, His378Ala and Glu402Ala were
120 completely lack of peptidase activity. We referred these three mutants to as ΔACE2-Fc (Δ: loss-of-activity)
121 and considered them as candidate variants emerged from the screen.

122 **Binding affinities of individual ACE2-Fc mutants to SARS-CoV-2 receptor-binding domain**

123 Next, we performed binding assays using individual variants against purified spike RBD protein. As
124 expected, all mutants displayed similar levels of binding to viral RBD, considering the relatively minor
125 changes from the point mutations made to ACE2-Fc (**Fig3**). Overall, the wild-type protein showed the highest
126 binding affinity, whereas all three Zn^{2+}-binding site mutants, His374Ala, His378Ala and Glu402Ala, had the
127 lowest affinities to RBD. This is consistent with the expectation that the ion pocket is in proximity to the viral
128 binding site on ACE2 (**Fig1C**), and also that changing ion-binding can potentially induce structurally instability
129 of the protein. In contrast, Arg273Ala mutant of the substrate-binding pocket, which showed complete loss-
130 of-activity towards all three substrates, is situated on the distal lobe and is less likely to affect desired viral
131 binding.

132 **Competitive inhibition of pseudotyped viral transduction by R273A, H378A and E402A mutants of**
133 **ΔACE2-Fc**

134 ΔACE2-Fc Arg273Ala, His378Ale and Glu402Ala, and wild-type ACE2-Fc proteins were further tested for
135 their antiviral potency. We conducted a series of viral inhibition assays using a pseudotyped reporter virus
136 decorated with SARS-CoV-2 spike protein. The virus was able to transduce HEK293 cells that express full-

137 length receptor ACE2 (See Methods). Each of the four ACE2-Fc variants in a range of concentrations was
138 added to culture medium to test the potential of viral inhibition. As expected, all variants showed similar
139 levels of efficacy to block pseudoviral transduction (**Fig4A**), with wild-type ACE2-Fc had a leading IC_{50} of 0.13
140 µg/mL, followed by His378Ala, Arg273Ala and Glu402Ala with their IC_{50}s of 0.16 µg/mL, 0.19 µg/mL and 0.25
141 µg/mL, respectively (**Fig4B**).

142 **Pharmacokinetics of lead ΔACE2-Fc proteins**

143 We have previously shown the in vivo longevity of mouse ACE2-Fc, as well as the fact that mouse FcRn
144 recognizes human Fc(Liu et al., 2018). Here we intravenously injected the ACE2-Fc variants in mice and
145 measured pharmacokinetics of biologics. All three ΔACE2-Fc and their wild-type control exhibited long half-
146 lives in the range between 52.61 hrs and 69.88 hrs (**Fig5**), consistent with the expectation for Fc-fusion
147 proteins.

148

149 **Discussions**

150 In searching for potential therapeutic antivirals for treatment of SARS-CoV-2, our study followed a design
151 strategy of screening for ACE2-Fc variants of having an exclusive SARS-CoV-2 affinity with the absence of
152 enzymatic activity towards ACE2's vasoactive substrates. Based on the structure of ACE2's catalytic center,
153 we selected a total of 9 residues to be individually replaced with alanine. These included 3 residues with
154 their side chains binding to divalent cation and 6 residues that line the substrate pocket. We used a
155 surrogate fluorogenic substrate as well as two physiological substrates of ACE2 in reactions and discovered
156 an unexpected substrate-dependent inactivation among individual mutants of ACE2-Fc. The screening
157 results identified three loss-of-activity variants (ΔACE2-Fc), one with a mutation of substrate-binding site
158 and two others having impairment of cation-binding. All these lead candidates maintained their binding
159 capacity towards SARS-CoV-2 spike protein and inhibited the transduction of a pseudotyped reporter virus.

160 One of the main benefits of ACE2-Fc fusion construction is its long-acting time as compared to
161 recombinant ACE2 without the tag(Liu et al., 2018). It is expected to provide important assurance of
162 sufficient drug levels to counteract the fluctuating levels of virions in patients, particularly during viremia.
163 Based on clinical knowledge of Fc-tagged Factor VIII (ELOCTATE®) used in hemophilia A patients, dosing at 3-
164 5 day intervals is sufficient to maintain a high blood level of the drug (US FDA recommendation).

165 The structural arrangement of ACE2-Fc resembles that of an antibody, with the replacement of antigen-
166 binding Fab portion of antibody with ACE2 to bind SARS-CoV-2 spike. Meanwhile, the Fc portion can
167 potentially induce immunological clearance of the virus, which, together in a fusion with ACE2, may be an
168 effective immunoadhesin(Ashkenazi & Chamow, 1997; Kruse, 2020) to trigger complement activation,
169 antibody-mediated cytotoxicity, and agglutination of targets. With respect to the potential antibody-like
170 benefits of ACE2-Fc, we compare our overall strategy with existing CD4 immunoadhesin (termed PRO 542)
171 that has existing clinical data for the treatment of HIV infection(Chamow et al., 1992; Fletcher et al., 2007;
172 Jacobson et al., 2004; Jacobson et al., 2000; Shearer et al., 2000). PRO 542 (CD4-IgG2/Fc with CD4 targeting
173 HIV gp120) antiviral is a tetravalent fusion protein using the constant region of IgG2 as opposed to IgG1 of
174 ACE2-Fc. One notable difference is that IgG2 has extremely low affinity to FcγRs on phagocytic cells, while
175 both IgG1 and IgG2 can activate complement. With regard to our proof-of-principle study of ACE2-Fc as
176 candidate antiviral drugs, it is important to point out that in terms of choices of the Fc tag, there are
177 alternative strategies in recombinant construction. Nevertheless, the inclusion of immunoadhesin potentials
178 of the antiviral may have caveats. While it may certainly boost immune clearance of the virus, such as
179 through FcγR's selective binding of clustered Fc, it may also elevate complement and cytokine responses to
180 further aggravate the inflammation. Although these adverse side effects can be mitigated through
181 modifications of the Fc domain, the ultimate therapeutic effects in the context of individual patients'
182 conditions can only be determined through rigorous clinical studies.

183 With regard to drug toxicity, our mouse study of repeated doses of ACE2-Fc in mice had showed the
184 biologic to be well tolerated for up to two months(Liu et al., 2018). However, we cannot extrapolate that its
185 will also be safe COVID-19 patients. As we consider it is not a simple neutralizing agent of the virus, its
186 bifurcated ACE2 head groups can possibly trigger agglutination of the virus that can potentially aggravate
187 the hypercoagulable state, making the drug less tolerable in these conditions.

188 From the perspective of recombinant manufacturing, there are challenges ahead for the simple fact that
189 ACE2-Fc is a large protein (~130 kDa as a monomer and ~260 kDa as a dimer). Furthermore, cocrystal
190 structures of ACE2 with an inhibitor showed large movements of the two lobes as compared to the Apo
191 structures(Towler et al., 2004), suggesting an intrinsic instability of ACE2 protein. Also of note is an earlier
192 study by Lei et al using double mutations of His374 and His378 of the zinc-binding pocket for neutralization
193 of SARS-CoV-2(Lei et al., 2020). However, the ion is important in maintaining protein structure and stability
194 of metallopeptidases(Fridrich, Karmilin, & Stocker, 2016) (McCall, Huang, & Fierke, 2000; Namuswe & Berg,
195 2012). This double mutation, as well as our His378Ala and Glu402Ala single mutations of the zinc-binding

196 pocket may potentially suffer protein instability problems. On the other hand, Arg273Ala mutant that is
197 predicted to change the substrate pocket will likely have a milder impact on overall protein stability, which is
198 an important parameter in pharmaceutical production.

199

200 **Materials and Methods**

201 **Construction of ACE2-Fc mutant plasmids**

202 DNA sequence encoding the ectodomain of human ACE2 (aa 1-740) was cloned from a human kidney
203 cDNA library. DNA encoding human Fc of IgG1 has been described previously(Liu et al., 2018). An in-frame
204 fusion between ACE2 and Fc was constructed in pcDNA3 vector (Invitrogen, Carlsbad, CA). Site-directed
205 mutagenesis by PCR was performed to create the panel of ACE2-Fc mutants. All mutants were confirmed by
206 sequencing.

207 **Recombinant protein expression and purification**

208 The workflow for generating recombinant ACE2-Fc variants was similar to what had been reported
209 before(Liu et al., 2018). Briefly, HEK293 cells were transfected with individual ACE2-Fc variants by standard
210 polyethylenimine (PEI) method. In transgene transfection studies, on day two of transfection cells were
211 switched to serum-free DMEM. On day four, the culture media were harvested by centrifugation, and
212 further concentrated using Amico Ultra Filters (Millipore, Billerica, MA). ACE2-Fc proteins were then purified
213 by size-exclusion chromatography (SEC) using Superdex 200 Increase column (GE healthcare, Chicago, IL)
214 and stored at -80°C until used in experiments.

215 ΔACE2-Fc Arg273Ala, His378Ala and Glu402Ala, and wild-type ACE2-Fc selected for scaled production
216 were produced from clonal stable-expressing cells. The general method was described previously(Liu et al.,
217 2018). Following plasmid transfection of HEK293 cells, the cells were selected under 1 mg/mL G418 (Thermo
218 Fisher Scientific, Waltham, MA) for ~14 days until isolated cell colonies appeared in the dishes. Individual
219 cell clones were seeded into 96-well plates. When cells reached 50-100% density in the wells, the culture
220 media were tested for their ACE2-Fc contents using a custom ELISA (anti-ACE2 antibody [Abcam, Cambridge,
221 MA] for capturing and anti-human IgG-Fc-HRP [SouthernBiotech, Birmingham, AL] for detection). Clones
222 with the highest expression of recombinant ACE2-Fc variants were selected, and individually expanded to
223 five 150 mm dishes. Once reached ~90% confluency, the cultures were switched to serum-free DMEM
224 medium. After 4-5 days the culture media were harvested, and further concentrated using a VIVAFLOW 200

225 filtration system (100,000 MWCO by Sartorius, Stonehouse, UK). Recombinant ACE2-Fc proteins were
226 purified using SEC as described above.

227 **ACE2 peptidase activity measured using surrogate Mca-APK(Dnp)**

228 ACE2-Fc peptidase activity assay using surrogate fluorogenic substrate Mca-APK(Dnp) (Enzo Life Sciences,
229 Farmingdale, NY) was performed in black microtiter plates. The reaction buffer contained 50 mM 4-
230 morpholineethanesulfonic acid, pH = 6.5, 300 mM NaCl, 10 µM $ZnCl_2$, 0.01% Triton X-100 and 20 µM of
231 Ma-APK(Dnp). The total reaction volume was 100 µL at room temperature and the duration of the reactions
232 were 30 min. Peptidase activities were calculated as fluorescence intensity at 320 nm excitation and 420 nm
233 emission wavelength.

234 **ACE2 peptidase activity measured using physiological substrates of AngII and apelin-13**

235 We described the method previously and referred to the workflow as Phenylalanine Assay, which was
236 tested using AngII and apelin-13 as substrates in reactions with ACE2(Liu et al., 2017). It involves two
237 coupled reactions, hydrolysis of the C-terminus phenylalanine residues from the substrates by ACE2 catalysis
238 and the measurement of free amino acid phenylalanine using yeast enzyme of phenylalanine ammonia lyase
239 (PAL) in a colorimetric assay (supplementary Figure S2).

240 The reactions were carried out using indicated concentrations of ACE2-Fc proteins together with either
241 AngII or apelin-13 at indicated concentrations in reaction buffer containing 20 mM Tris-HCl, pH = 7.4,
242 136 mM NaCl and 10 µM $ZnCl_2$. The first reaction was proceeded at 37°C after 30 min before stopped by
243 80°C heat inactivation for 5 min. The second reaction used a phenylalanine detection kit (Sigma-Aldrich, St.
244 Louis, MO). 1 µL enzyme mix and 1 µL developer from the kit were added to the above reaction, which was
245 allowed to proceed for 60 min at room temperature. Fluorescence intensity was measured at 535 nm
246 excitation and 585 nm emission wavelength, and all reactions were performed in triplicate.

247 **SARS-CoV-2 RBD binding assay**

248 Recombinant viral RBD protein was purchased from Sino Biological (Beijing, China). ELISA wells were
249 precoated with either PBS as controls or 100 ng/well of RBD protein. Serial concentrations of individual
250 ACE2-Fc variants were added to the wells. After overnight incubation at 4℃, the wells were washed three
251 times with TBST buffer before HRP-conjugated anti-human IgG-Fc secondary antibody was added. HRP
252 reactions were developed with TMB substrate and the binding strength derived from OD450 (nm) readings

253 of the reactions. The EC50 values were determined by log(agonist) vs. response nonlinear regression fit
254 analysis (GraphPad Prism).

255 **Inhibition of viral transduction with purified ΔACE2-Fc mutants**

256 Spike (SARS-CoV-2) pseudotyped lentivirus with luciferase reporter gene was purchased from BPS
257 Bioscience (San Diego, CA). The virus was used to transduce HEK293 with stable expression of receptor full-
258 length ACE2. The stable cell line was created from plasmid expressing full-length human ACE2 in pcDNA3
259 vector. Followed a similar procedure for generating ACE2-Fc clones, stable HEK293 clones with receptor
260 ACE2 expression was identified using immune detection of ACE2 in the cells. The ACE2-HEK293 cells were
261 seeded at a density of 10,000 cells per well into 96-well cell culture microplate one day before transduction.
262 To test inhibition of viral transduction, 5 µL pseudotyped lentivirus were preincubated with 5 µL vehicle or
263 serially diluted ACE2-Fc variants at 37 °C for 1 h add then added into the cells. After overnight incubation,
264 the cells were refed with fresh medium and incubated for another 36 hours. Luciferase activity was
265 measured using ONE-Glo™ Luciferase Assay System according to the manufacture's protocol (Promega,
266 Madison, WI). The IC50 values were determined by log(inhibitor) vs. response nonlinear regression fit
267 analysis (GraphPad Prism).

268 **ACE2-Fc pharmacokinetics in mice**

269 The general method for pharmacokinetic measurements were described previously(Liu et al., 2018).
270 Briefly, a bolus intravenous injection of ACE2-Fc proteins (0.5mg/kg body weight) performed in female
271 BALB/c mice. Subsequently, serial blood samples were collected from tail bleeding at indicated time points.
272 Collected blood samples were left undisturbed on ice, and sera were isolated by centrifugation at 6000 x *g*
273 for 10 minutes at 4°C. The levels of ACE2-Fc in the sera were measured by ELISA using anti-ACE2 capturing
274 antibody and anti-human IgG-Fc-HRP antibody for detection as described above.

275 **Acknowledgements**

276 The design of the study was inspired by Dr. Robert Kruse's *F1000Research* article. We thank Drs. Danial
277 Batlle and Jan Wysocki for their insightful comments.

278 **Conflict of interest**: Jing Jin and Pan Liu have applied for a provisional patent of the ACE2-Fc mutants
279 described in the article.

280

281 **Figure legends**

Figure 1. Mutagenesis strategies for catalytic inactivation of ACE2. A. Schematic representation of chimeric ACE2-Fc. The ectodomain sequence from amino acid 19 to 740 of human ACE2 is fused to the N-terminus of Fc domain of human IgG1, which forms a dimer via disulfide bridges (blue lines). The overall plan was to make individual point mutations (denoted as stars) of the catalytic site to inactivate the ACE2 peptidase activity. **B**. Mutant ACE2-Fc proteins, each carries a single alanine substitution of a selected residue, were produced by HEK-293 cells. As predicted, the proteins ran above the 250 kDa marker under nonreducing condition. **C**. The cocrystal structure (PDB: 6M0J) shows SARS-CoV-2 spike RBD binding of ACE2. ACE2 exists in a clam shell-like configuration holding a catalytic cleft between its proximal and distal lobes. A zinc ion resides within the proximal lobe of the cleft void. **D**. In an inhibitor (MLN-4760)-bound structure of ACE2 (PBD: 1R4L), the inhibitor induced a conformational change of the catalytic cleft to adapt a 'closed' configuration(Towler et al., 2004). **E**. Three proximal lobe residues H374, H378 and E402 formed interactions with the zinc ion. **F**. The side chains of six proximal and distal lobe residues, E145, R273, H345, P346, D368 and H505 (in green) formed direct interactions with inhibitor MLN-4760 (in magentas).

Figure 2. Substrate-dependent inactivation of ACE2-Fc peptidase among ACE2-Fc mutants. Three peptide substrates were tested in catalytic reactions with ten individual variants of ACE2-Fc (wild-type and 9 mutants). The reactions were carried out in two different ways. Left panels: the reactions were performed using a high amount of purified ACE2-Fc enzyme (100 ng) with varying concentrations of the substrates between 0.39 µM and 200 µM (x-axis). Right panels: a lower dose of 10 ng ACE2-Fc was incubated with a fixed amount of 2 nmole of Mca-APK(Dnp) or 10 nmole of AngII/Apelin-13. Reactions proceeded for a standard length of time of 20 min. **A**. Surrogate fluorogenic substrate Mca-AP↓K(Dnp) was tested (↓: cleavage site). ACE2-Fc peptidase activities were compared between wild-type and mutants. Seven out of the nine mutants showed a completely loss-of-activity. **B**. When AngII was used in reactions with the ACE-2-Fc panel, DRVYIHP↓F of AngII sequence was cleaved by ACE2, releasing a Phe/F. The assay detected the generation of amino acid Phe/F as the results of ACE2-Fc activity. **C**. Similar to AngII, Apelin-13 was cleaved by ACE2 between the proline(P)-phenylalanine (F) bond in its sequence, Pyr-RPRLSHKGPMP↓F. The rates of Phe/F release from the reactions were detected.

Figure 3. Binding affinities of individual ACE2-Fc variants to RBD of SARS-CoV-2 spike protein. A. A fixed amount of recombinant viral RBD protein was coated to an ELISA plate (buffer coated well were used as controls). Wild-type and nine mutants of ACE2-Fc were added to the wells at varying concentrations between 0.5 ng/mL and 1200 ng/mL (x-axis). Binding was determined by the difference in signal intensity between the RBD-coated and the corresponding control wells. **B**. While all variants of ACE2-Fc exhibited affinity to viral RBD protein, there were differences in their calculated IC_{50} values.

Figure 4. **Inhibition of a pseudotyped virus by wild-type ACE2-Fc and ΔACE2-Fc variants**. **A**. The transduction activity of a pseudotyped virus expressing SARS-CoV-2 spike protein to HEK293 cells expressing receptor ACE2 was measured through a firefly luciferase reporter. The cell transduction assays were performed in the presence of various concentrations of individual ACE2-Fc variants. **B**. IC_{50} values were calculated based on calculated ACE2-Fc concentrations needed to inhibit 50% reporter activity.

Figure 5. **Pharmacokinetics of wild-type ACE2-Fc and ΔACE2-Fc variants**. **A**. After a bolus *i.v.* injection of the listed ACE2-Fc variants in mice (n=3), drug concentration in blood was monitored over a period time. **B**. $t_{(1/2)}$ values of individual biologics were calculated by GraphPad Prism software.

References

Ashkenazi, A., & Chamow, S. M. (1997). Immunoadhesins as research tools and therapeutic agents. *Curr Opin Immunol, 9*(2), 195-200. doi:10.1016/s0952-7915(97)80135-5

Bavishi, C., Maddox, T. M., & Messerli, F. H. (2020). Coronavirus Disease 2019 (COVID-19) Infection and Renin Angiotensin System Blockers. *JAMA Cardiol*. doi:10.1001/jamacardio.2020.1282

Bosmuller, H., Traxler, S., Bitzer, M., Haberle, H., Raiser, W., Nann, D., . . . Fend, F. (2020). The evolution of pulmonary pathology in fatal COVID-19 disease: an autopsy study with clinical correlation. *Virchows Arch*. doi:10.1007/s00428-020-02881-x

Cai, A., McClafferty, B., Benson, J., Ramgobin, D., Kalayanamitra, R., Shahid, Z., . . . Jain, R. (2020). COVID-19: Catastrophic Cause of Acute Lung Injury. *S D Med, 73*(6), 252-260. Retrieved from https://www.ncbi.nlm.nih.gov/pubmed/32580257

Chamow, S. M., Duliege, A. M., Ammann, A., Kahn, J. O., Allen, J. D., Eichberg, J. W., . . . Ashkenazi, A. (1992). CD4 immunoadhesins in anti-HIV therapy: new developments. *Int J Cancer Suppl, 7*, 69-72. Retrieved from https://www.ncbi.nlm.nih.gov/pubmed/1428410

Chan, K. K., Dorosky, D., Sharma, P., Abbasi, S. A., Dye, J. M., Kranz, D. M., . . . Procko, E. (2020). Engineering human ACE2 to optimize binding to the spike protein of SARS coronavirus 2. *Science*. doi:10.1126/science.abc0870

Danser, A. H. J., Epstein, M., & Batlle, D. (2020). Renin-Angiotensin System Blockers and the COVID-19 Pandemic: At Present There Is No Evidence to Abandon Renin-Angiotensin System Blockers. *Hypertension, 75*(6), 1382-1385. doi:10.1161/HYPERTENSIONAHA.120.15082

Fletcher, C. V., DeVille, J. G., Samson, P. M., Moye, J. H., Jr., Church, J. A., Spiegel, H. M., . . . Pediatric Aids Clinical Trials Group, P. S. G. (2007). Nonlinear pharmacokinetics of high-dose recombinant fusion protein CD4-IgG2 (PRO 542) observed in HIV-1-infected children. *J Allergy Clin Immunol, 119*(3), 747-750. doi:10.1016/j.jaci.2006.10.045

Fridrich, S., Karmilin, K., & Stocker, W. (2016). Handling Metalloproteinases. *Curr Protoc Protein Sci, 83*, 21 16 21-21 16 20. doi:10.1002/0471140864.ps2116s83

Guo, J., Huang, Z., Lin, L., & Lv, J. (2020). Coronavirus Disease 2019 (COVID-19) and Cardiovascular Disease: A Viewpoint on the Potential Influence of Angiotensin-Converting Enzyme Inhibitors/Angiotensin Receptor Blockers on Onset and Severity of Severe Acute Respiratory Syndrome Coronavirus 2 Infection. *J Am Heart Assoc, 9*(7), e016219. doi:10.1161/JAHA.120.016219

Guzik, T. J., Mohiddin, S. A., Dimarco, A., Patel, V., Savvatis, K., Marelli-Berg, F. M., . . . McInnes, I. B. (2020). COVID-19 and the cardiovascular system: implications for risk assessment, diagnosis, and treatment options. *Cardiovasc Res*. doi:10.1093/cvr/cvaa106

Hemnes, A. R., Rathinasabapathy, A., Austin, E. A., Brittain, E. L., Carrier, E. J., Chen, X., . . . West, J. (2018). A potential therapeutic role for angiotensin-converting enzyme 2 in human pulmonary arterial hypertension. *Eur Respir J, 51*(6). doi:10.1183/13993003.02638-2017

Hoffmann, M., Kleine-Weber, H., Schroeder, S., Kruger, N., Herrler, T., Erichsen, S., . . . Pohlmann, S. (2020). SARS-CoV-2 Cell Entry Depends on ACE2 and TMPRSS2 and Is Blocked by a Clinically Proven Protease Inhibitor. *Cell, 181*(2), 271-280 e278. doi:10.1016/j.cell.2020.02.052

Imai, Y., Kuba, K., Rao, S., Huan, Y., Guo, F., Guan, B., . . . Penninger, J. M. (2005). Angiotensin-converting enzyme 2 protects from severe acute lung failure. *Nature, 436*(7047), 112-116. doi:10.1038/nature03712

Iwanaga, N., Cooper, L., Rong, L., Beddingfield, B., Crabtree, J., Tripp, R. A., & Kolls, J. K. (2020). Novel ACE2-IgG1 fusions with improved activity against SARS-CoV2. *bioRxiv*. doi:10.1101/2020.06.15.152157

Jacobson, J. M., Israel, R. J., Lowy, I., Ostrow, N. A., Vassilatos, L. S., Barish, M., . . . Olson, W. C. (2004). Treatment of advanced human immunodeficiency virus type 1 disease with the viral entry

371 inhibitor PRO 542. *Antimicrob Agents Chemother, 48*(2), 423-429. doi:10.1128/aac.48.2.423-
372 429.2004
373 Jacobson, J. M., Lowy, I., Fletcher, C. V., O'Neill, T. J., Tran, D. N., Ketas, T. J., . . . Israel, R. J. (2000).
374 Single-dose safety, pharmacology, and antiviral activity of the human immunodeficiency virus
375 (HIV) type 1 entry inhibitor PRO 542 in HIV-infected adults. *J Infect Dis, 182*(1), 326-329.
376 doi:10.1086/315698
377 Khan, A., Benthin, C., Zeno, B., Albertson, T. E., Boyd, J., Christie, J. D., . . . Lazaar, A. L. (2017). A pilot
378 clinical trial of recombinant human angiotensin-converting enzyme 2 in acute respiratory
379 distress syndrome. *Crit Care, 21*(1), 234. doi:10.1186/s13054-017-1823-x
380 Kruse, R. L. (2020). Therapeutic strategies in an outbreak scenario to treat the novel coronavirus
381 originating in Wuhan, China. *F1000Res, 9*, 72. doi:10.12688/f1000research.22211.2
382 Lan, J., Ge, J., Yu, J., Shan, S., Zhou, H., Fan, S., . . . Wang, X. (2020). Structure of the SARS-CoV-2 spike
383 receptor-binding domain bound to the ACE2 receptor. *Nature, 581*(7807), 215-220.
384 doi:10.1038/s41586-020-2180-5
385 Lei, C., Qian, K., Li, T., Zhang, S., Fu, W., Ding, M., & Hu, S. (2020). Neutralization of SARS-CoV-2 spike
386 pseudotyped virus by recombinant ACE2-Ig. *Nat Commun, 11*(1), 2070. doi:10.1038/s41467-020-
387 16048-4
388 Liu, P., Wysocki, J., Serfozo, P., Ye, M., Souma, T., Batlle, D., & Jin, J. (2017). A Fluorometric Method of
389 Measuring Carboxypeptidase Activities for Angiotensin II and Apelin-13. *Sci Rep, 7*, 45473.
390 doi:10.1038/srep45473
391 Liu, P., Wysocki, J., Souma, T., Ye, M., Ramirez, V., Zhou, B., . . . Jin, J. (2018). Novel ACE2-Fc chimeric
392 fusion provides long-lasting hypertension control and organ protection in mouse models of
393 systemic renin angiotensin system activation. *Kidney Int, 94*(1), 114-125.
394 doi:10.1016/j.kint.2018.01.029
395 Lumbers, E. R., Delforce, S. J., Pringle, K. G., & Smith, G. R. (2020). The Lung, the Heart, the Novel
396 Coronavirus, and the Renin-Angiotensin System; The Need for Clinical Trials. *Front Med*
397 *(Lausanne), 7*, 248. doi:10.3389/fmed.2020.00248
398 McCall, K. A., Huang, C., & Fierke, C. A. (2000). Function and mechanism of zinc metalloenzymes. *J Nutr,*
399 *130*(5S Suppl), 1437S-1446S. doi:10.1093/jn/130.5.1437S
400 Mehra, M. R., Desai, S. S., Kuy, S., Henry, T. D., & Patel, A. N. (2020). Cardiovascular Disease, Drug
401 Therapy, and Mortality in Covid-19. *N Engl J Med, 382*(25), e102. doi:10.1056/NEJMoa2007621
402 Menter, T., Haslbauer, J. D., Nienhold, R., Savic, S., Hopfer, H., Deigendesch, N., . . . Tzankov, A. (2020).
403 Post-mortem examination of COVID19 patients reveals diffuse alveolar damage with severe
404 capillary congestion and variegated findings of lungs and other organs suggesting vascular
405 dysfunction. *Histopathology*. doi:10.1111/his.14134
406 Monteil, V., Kwon, H., Prado, P., Hagelkruys, A., Wimmer, R. A., Stahl, M., . . . Penninger, J. M. (2020).
407 Inhibition of SARS-CoV-2 Infections in Engineered Human Tissues Using Clinical-Grade Soluble
408 Human ACE2. *Cell, 181*(4), 905-913 e907. doi:10.1016/j.cell.2020.04.004
409 Namuswe, F., & Berg, J. M. (2012). Secondary interactions involving zinc-bound ligands: roles in
410 structural stabilization and macromolecular interactions. *J Inorg Biochem, 111*, 146-149.
411 doi:10.1016/j.jinorgbio.2011.10.018
412 Noris, M., Benigni, A., & Remuzzi, G. (2020). The case of complement activation in COVID-19 multiorgan
413 impact. *Kidney Int*. doi:10.1016/j.kint.2020.05.013
414 Renu, K., Prasanna, P. L., & Valsala Gopalakrishnan, A. (2020). Coronaviruses pathogenesis,
415 comorbidities and multi-organ damage - A review. *Life Sci, 255*, 117839.
416 doi:10.1016/j.lfs.2020.117839
417 Rossi, G. P., Sanga, V., & Barton, M. (2020). Potential harmful effects of discontinuing ACE-inhibitors and
418 ARBs in COVID-19 patients. *Elife, 9*. doi:10.7554/eLife.57278

Shang, J., Ye, G., Shi, K., Wan, Y., Luo, C., Aihara, H., . . . Li, F. (2020). Structural basis of receptor recognition by SARS-CoV-2. *Nature, 581*(7807), 221-224. doi:10.1038/s41586-020-2179-y

Shearer, W. T., Israel, R. J., Starr, S., Fletcher, C. V., Wara, D., Rathore, M., . . . Olson, W. C. (2000). Recombinant CD4-IgG2 in human immunodeficiency virus type 1-infected children: phase 1/2 study. The Pediatric AIDS Clinical Trials Group Protocol 351 Study Team. *J Infect Dis, 182*(6), 1774-1779. doi:10.1086/317622

Sommerstein, R., Kochen, M. M., Messerli, F. H., & Grani, C. (2020). Coronavirus Disease 2019 (COVID-19): Do Angiotensin-Converting Enzyme Inhibitors/Angiotensin Receptor Blockers Have a Biphasic Effect? *J Am Heart Assoc, 9*(7), e016509. doi:10.1161/JAHA.120.016509

South, A. M., Brady, T. M., & Flynn, J. T. (2020). ACE2 (Angiotensin-Converting Enzyme 2), COVID-19, and ACE Inhibitor and Ang II (Angiotensin II) Receptor Blocker Use During the Pandemic: The Pediatric Perspective. *Hypertension, 76*(1), 16-22. doi:10.1161/HYPERTENSIONAHA.120.15291

South, A. M., Diz, D. I., & Chappell, M. C. (2020). COVID-19, ACE2, and the cardiovascular consequences. *Am J Physiol Heart Circ Physiol, 318*(5), H1084-H1090. doi:10.1152/ajpheart.00217.2020

Sparks, M. A., South, A., Welling, P., Luther, J. M., Cohen, J., Byrd, J. B., . . . Hiremath, S. (2020). Sound Science before Quick Judgement Regarding RAS Blockade in COVID-19. *Clin J Am Soc Nephrol, 15*(5), 714-716. doi:10.2215/CJN.03530320

Stafford, E. G., Riviere, J. E., Xu, X., Kawakami, J., Wyckoff, G. J., & Jaberi-Douraki, M. (2020). Pharmacovigilance in patients with diabetes: A data-driven analysis identifying specific RAS antagonists with adverse pulmonary safety profiles that have implications for COVID-19 morbidity and mortality. *J Am Pharm Assoc (2003)*. doi:10.1016/j.japh.2020.05.018

Towler, P., Staker, B., Prasad, S. G., Menon, S., Tang, J., Parsons, T., . . . Pantoliano, M. W. (2004). ACE2 X-ray structures reveal a large hinge-bending motion important for inhibitor binding and catalysis. *J Biol Chem, 279*(17), 17996-18007. doi:10.1074/jbc.M311191200

Vaduganathan, M., Vardeny, O., Michel, T., McMurray, J. J. V., Pfeffer, M. A., & Solomon, S. D. (2020). Renin-Angiotensin-Aldosterone System Inhibitors in Patients with Covid-19. *N Engl J Med, 382*(17), 1653-1659. doi:10.1056/NEJMsr2005760

Walls, A. C., Park, Y. J., Tortorici, M. A., Wall, A., McGuire, A. T., & Veesler, D. (2020). Structure, Function, and Antigenicity of the SARS-CoV-2 Spike Glycoprotein. *Cell, 181*(2), 281-292 e286. doi:10.1016/j.cell.2020.02.058

Wang, Q., Zhang, Y., Wu, L., Niu, S., Song, C., Zhang, Z., . . . Qi, J. (2020). Structural and Functional Basis of SARS-CoV-2 Entry by Using Human ACE2. *Cell, 181*(4), 894-904 e899. doi:10.1016/j.cell.2020.03.045

Wrapp, D., Wang, N., Corbett, K. S., Goldsmith, J. A., Hsieh, C. L., Abiona, O., . . . McLellan, J. S. (2020). Cryo-EM structure of the 2019-nCoV spike in the prefusion conformation. *Science, 367*(6483), 1260-1263. doi:10.1126/science.abb2507

Yan, R., Zhang, Y., Li, Y., Xia, L., Guo, Y., & Zhou, Q. (2020). Structural basis for the recognition of SARS-CoV-2 by full-length human ACE2. *Science, 367*(6485), 1444-1448. doi:10.1126/science.abb2762

Zaim, S., Chong, J. H., Sankaranarayanan, V., & Harky, A. (2020). COVID-19 and Multiorgan Response. *Curr Probl Cardiol, 45*(8), 100618. doi:10.1016/j.cpcardiol.2020.100618

Zheng, Y. Y., Ma, Y. T., Zhang, J. Y., & Xie, X. (2020). COVID-19 and the cardiovascular system. *Nat Rev Cardiol, 17*(5), 259-260. doi:10.1038/s41569-020-0360-5

Zhou, F., Yu, T., Du, R., Fan, G., Liu, Y., Liu, Z., . . . Cao, B. (2020). Clinical course and risk factors for mortality of adult inpatients with COVID-19 in Wuhan, China: a retrospective cohort study. *Lancet, 395*(10229), 1054-1062. doi:10.1016/S0140-6736(20)30566-3

Zhou, P., Yang, X. L., Wang, X. G., Hu, B., Zhang, L., Zhang, W., . . . Shi, Z. L. (2020). A pneumonia outbreak associated with a new coronavirus of probable bat origin. *Nature, 579*(7798), 270-273. doi:10.1038/s41586-020-2012-7

A

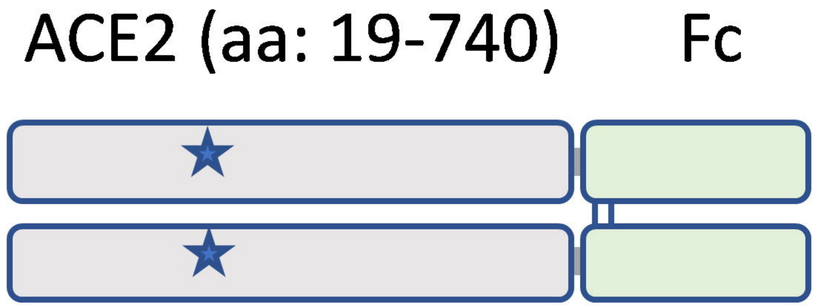
ACE2 (aa: 19-740)
Fc

B

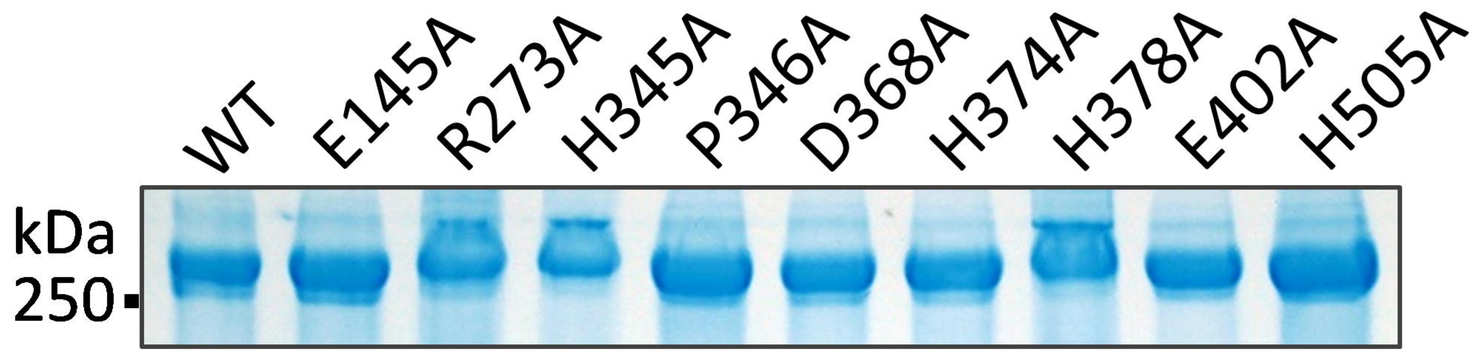
WT
E145A
R273A
H345A
P346A
D368A
H374A
H378A
E402A
H505A
kDa
250

C

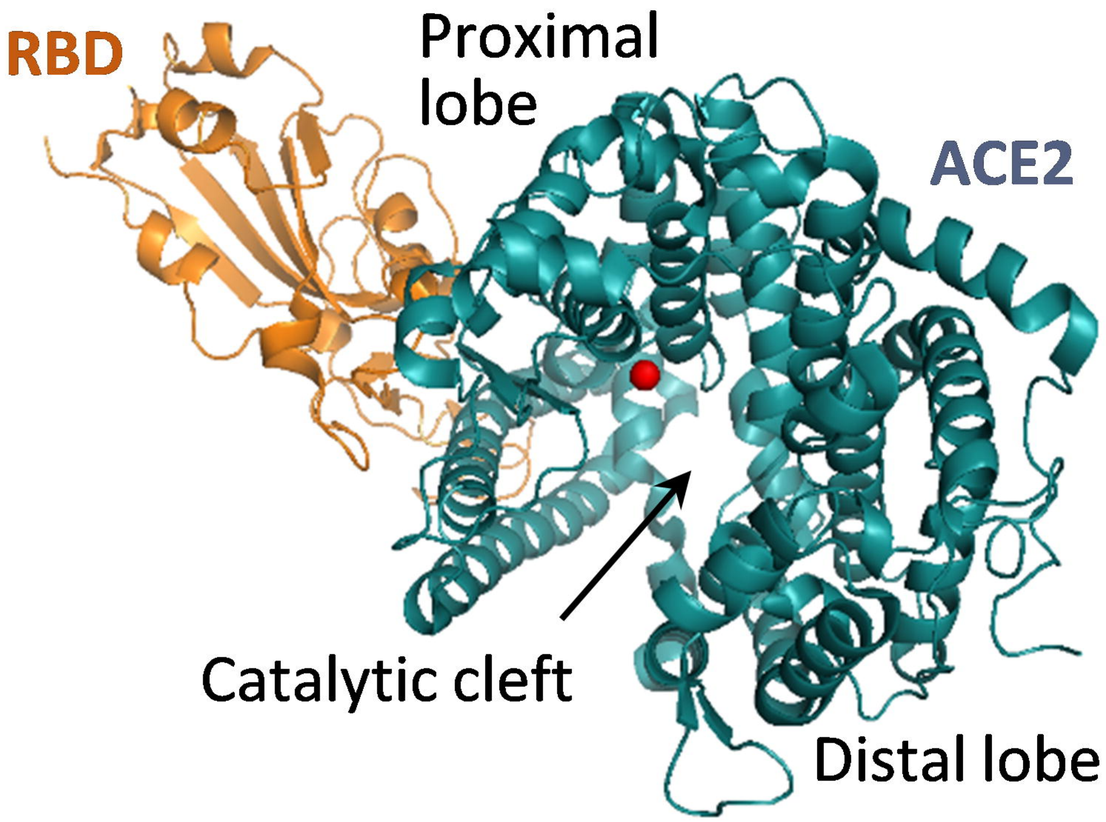
RBD
Proximal lobe
ACE2
Catalytic cleft
Distal lobe

D

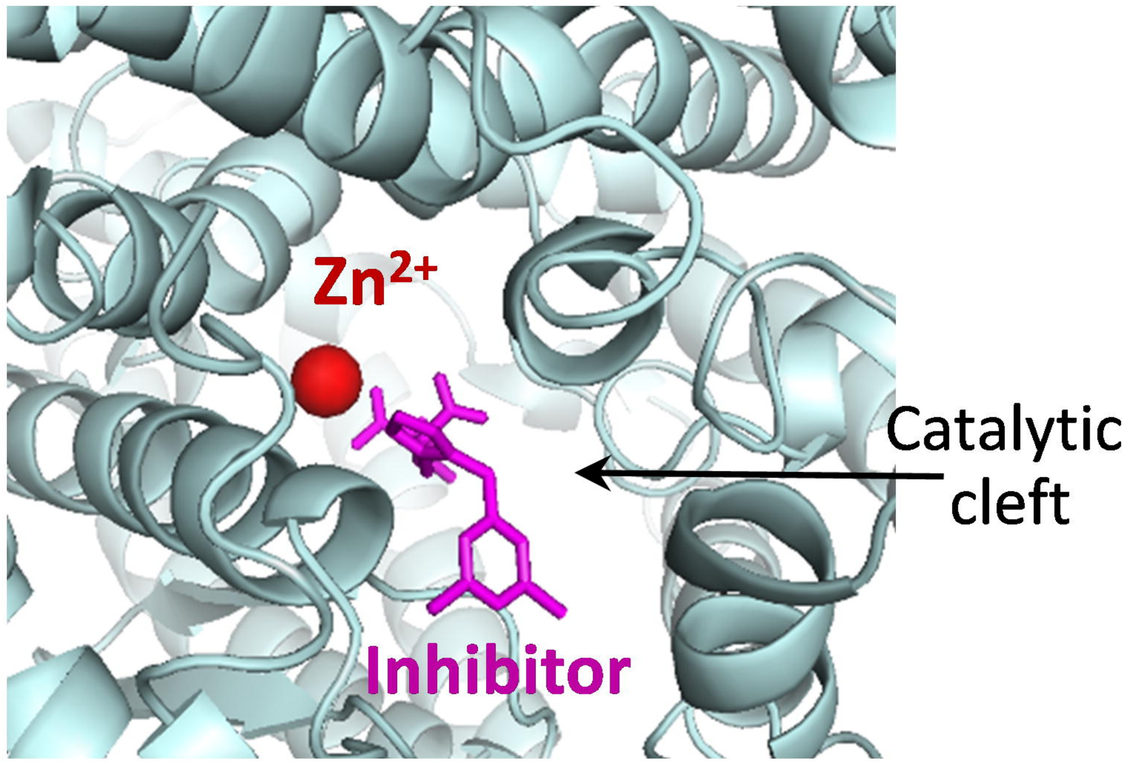
Zn^{2+}
Catalytic cleft
Inhibitor

E

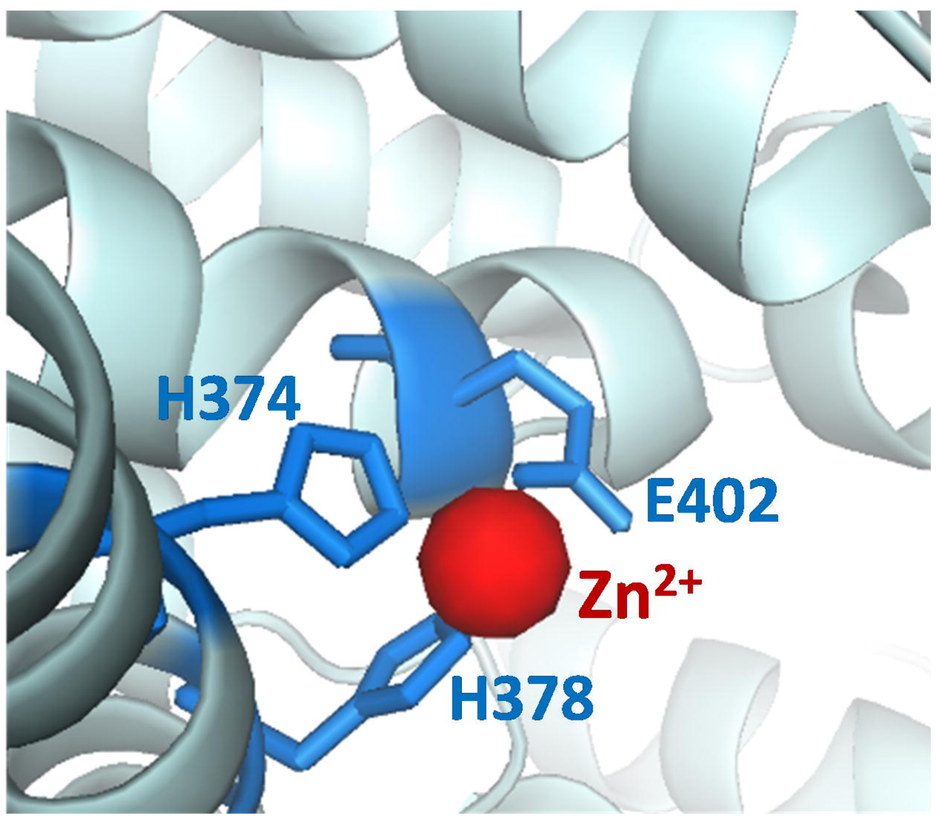
H374
E402
Zn^{2+}
H378

F

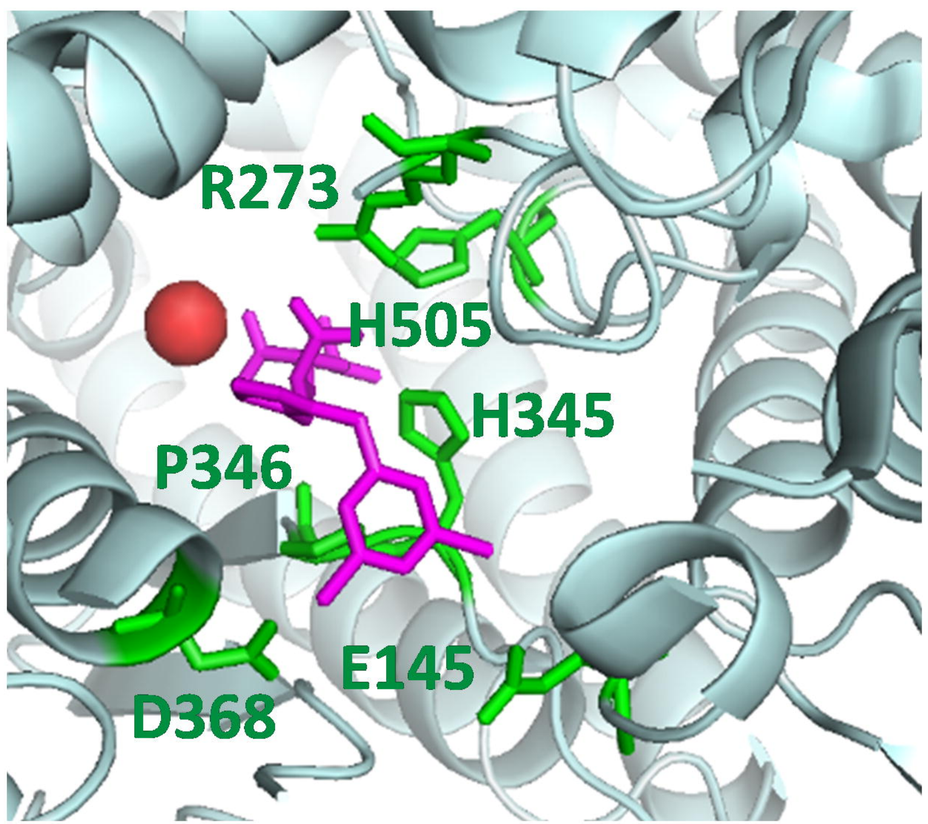
R273
H505
H345
P346
E145
D368

A

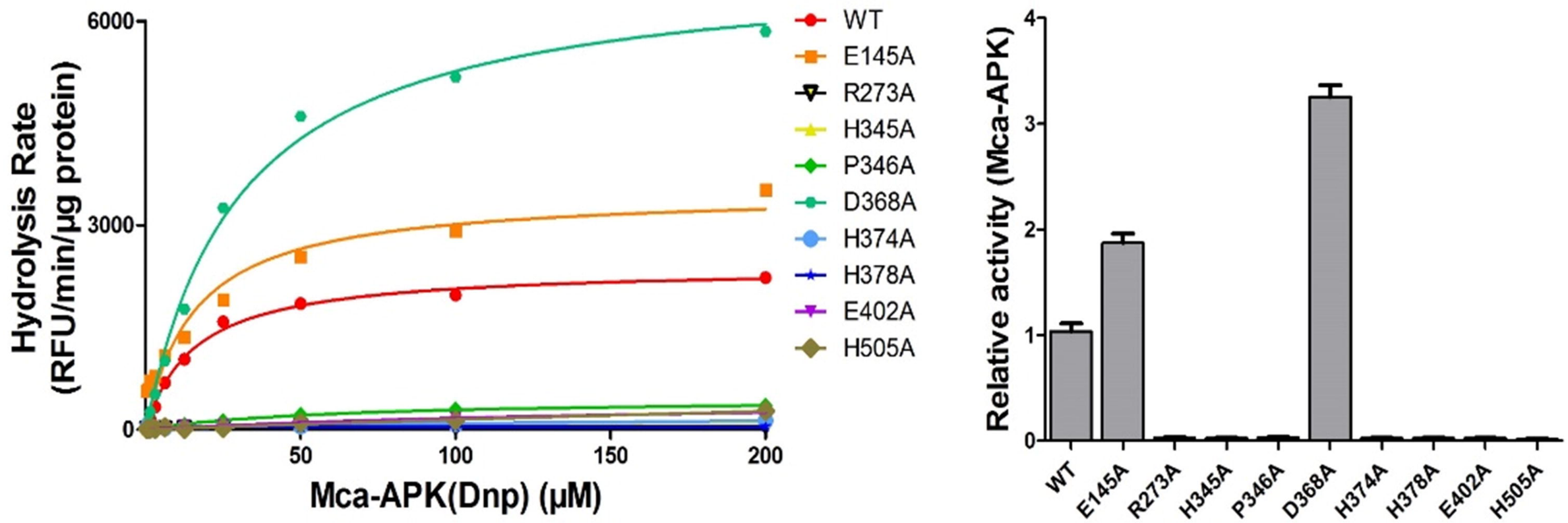
Hydrolysis Rate
(RFU/min/μg protein)
6000
3000
0
50
100
150
200
Mca-APK(Dnp) (μM)
WT
E145A
R273A
H345A
P346A
D368A
H374A
H378A
E402A
H505A
Relative activity (Mca-APK)
4
3
2
1
0
WT
E145A
R273A
H345A
P346A
D368A
H374A
H378A
E402A
H505A

B

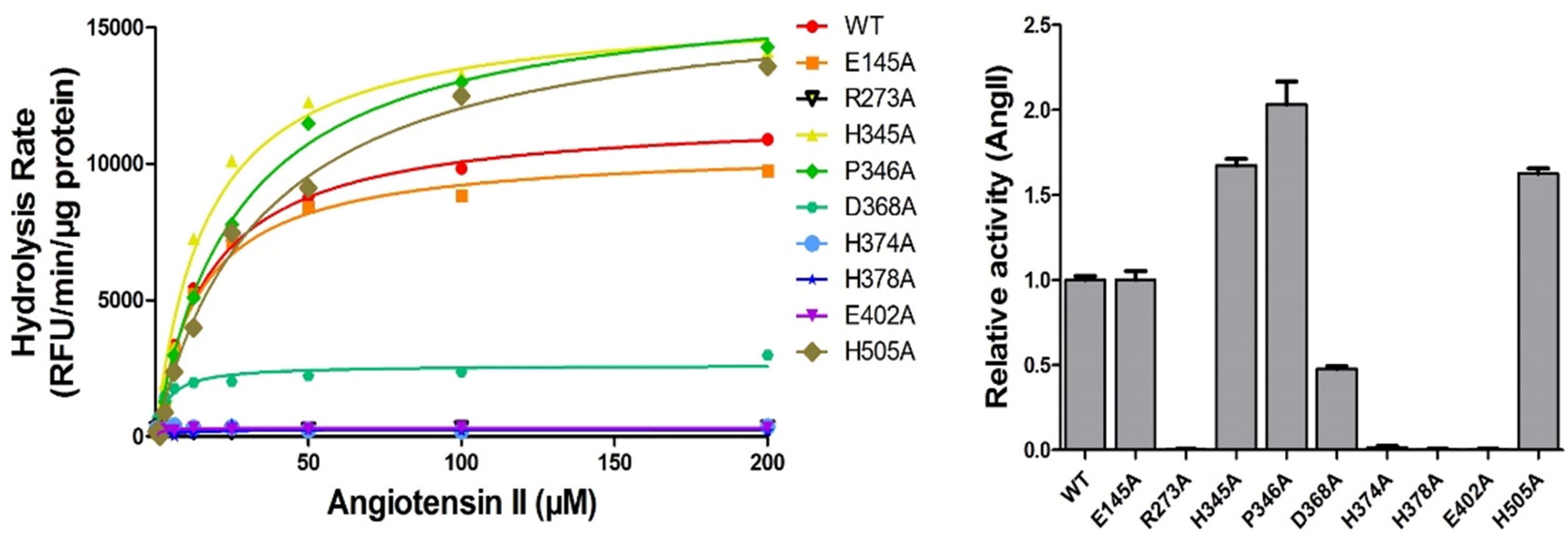
Hydrolysis Rate
(RFU/min/μg protein)
15000
10000
5000
0
50
100
150
200
Angiotensin II (μM)
WT
E145A
R273A
H345A
P346A
D368A
H374A
H378A
E402A
H505A
Relative activity (AngII)
2.5
2.0
1.5
1.0
0.5
0.0
WT
E145A
R273A
H345A
P346A
D368A
H374A
H378A
E402A
H505A

C

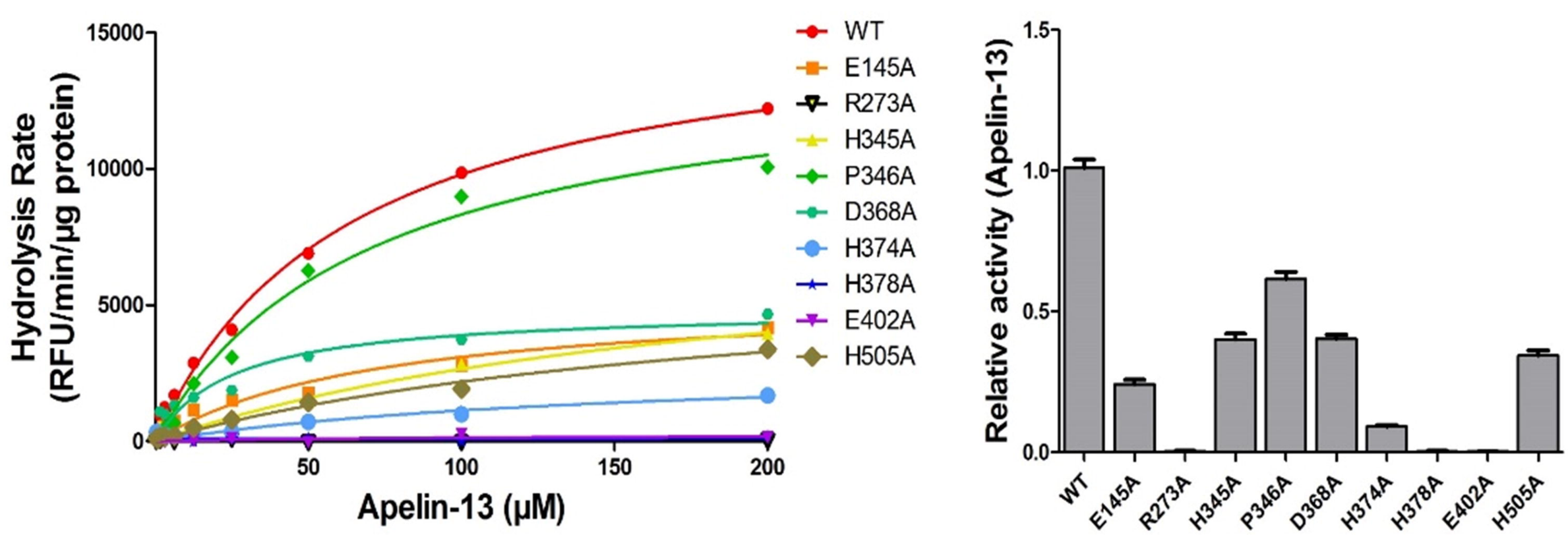
Hydrolysis Rate
(RFU/min/μg protein)
15000
10000
5000
0
50
100
150
200
Apelin-13 (μM)
WT
E145A
R273A
H345A
P346A
D368A
H374A
H378A
E402A
H505A
Relative activity (Apelin-13)
1.5
1.0
0.5
0.0
WT
E145A
R273A
H345A
P346A
D368A
H374A
H378A
E402A
H505A

A

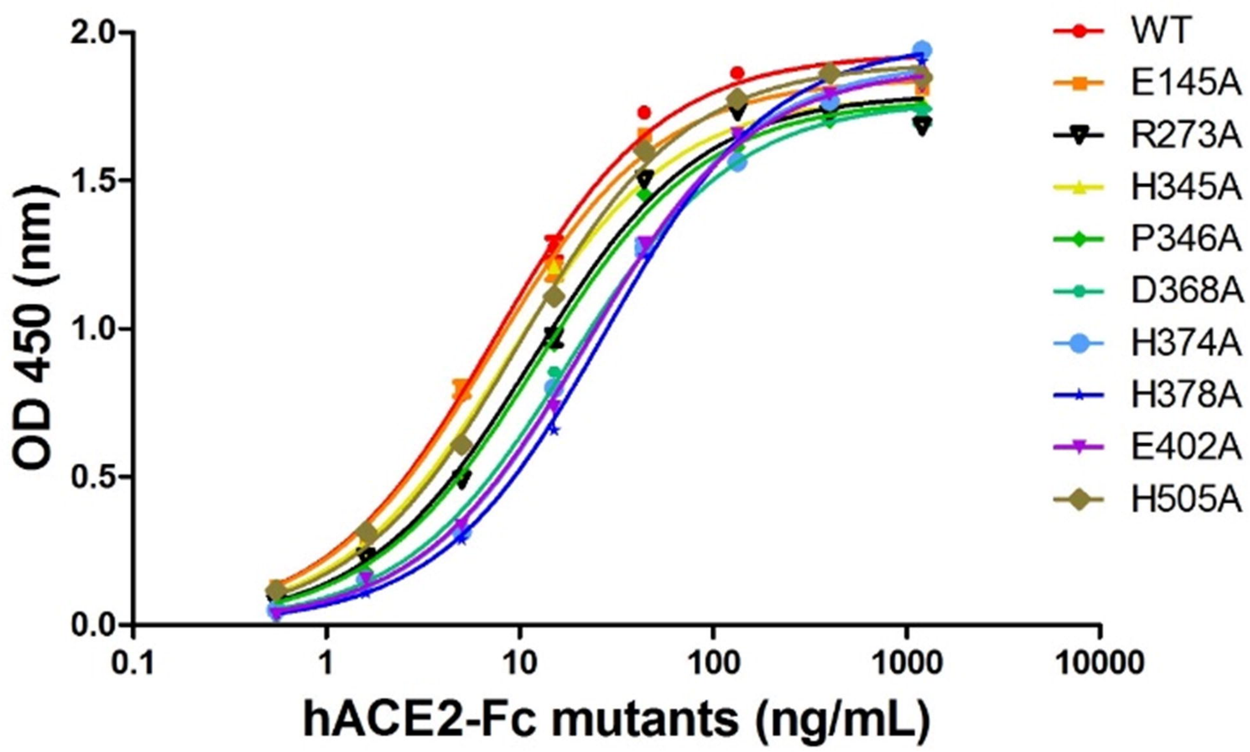

B

ACE2-Fc	EC_{50} (ng/mL)	ACE2-Fc	EC_{50} (ng/mL)
WT	7.3	D368A	16.7
E145A	7.2	H374A	23.1
R273A	12.6	H378A	26.9
H345A	8.2	E402A	21.8
P346A	11.9	H505A	11.3

A

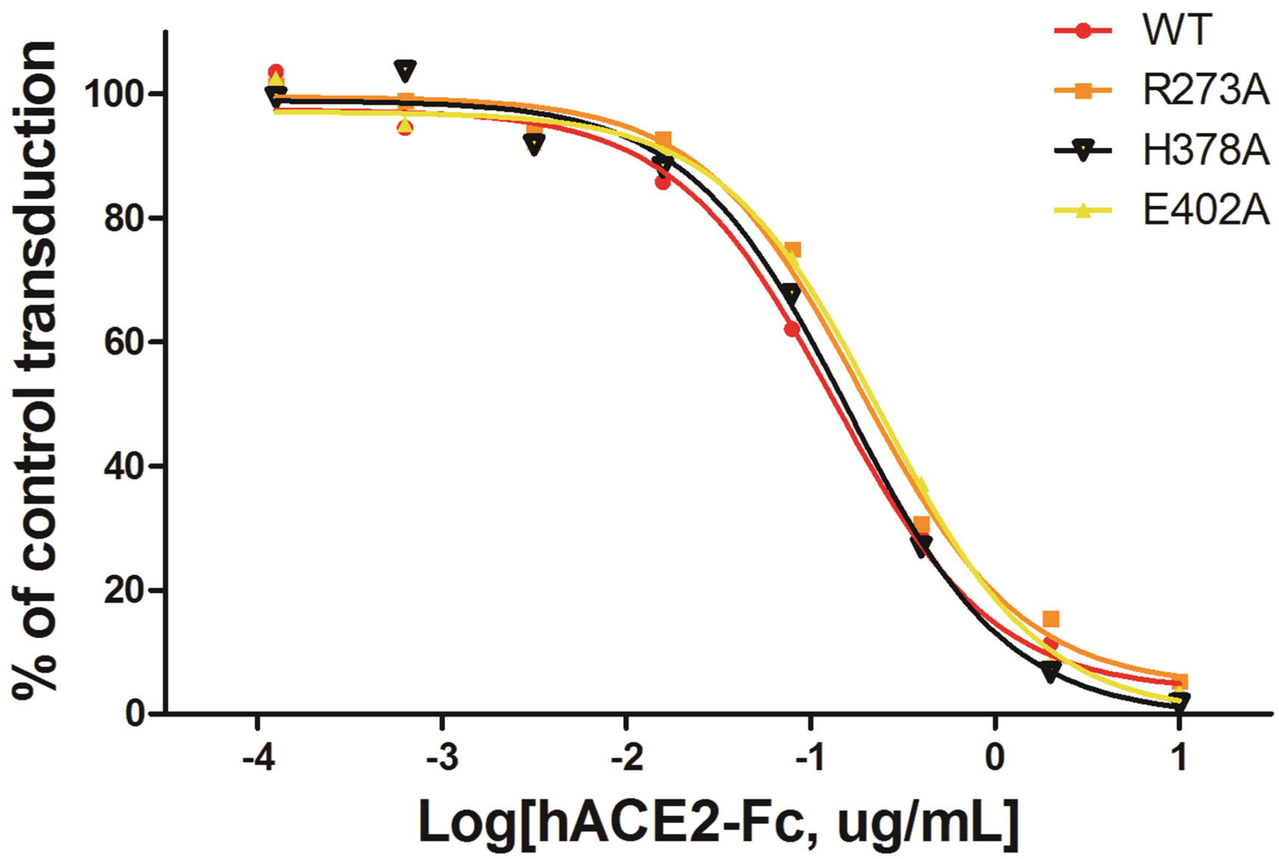

B

ACE2-Fc	IC_{50} (ug/mL)
WT	0.13
R273A	0.19
H378A	0.16
E402A	0.24

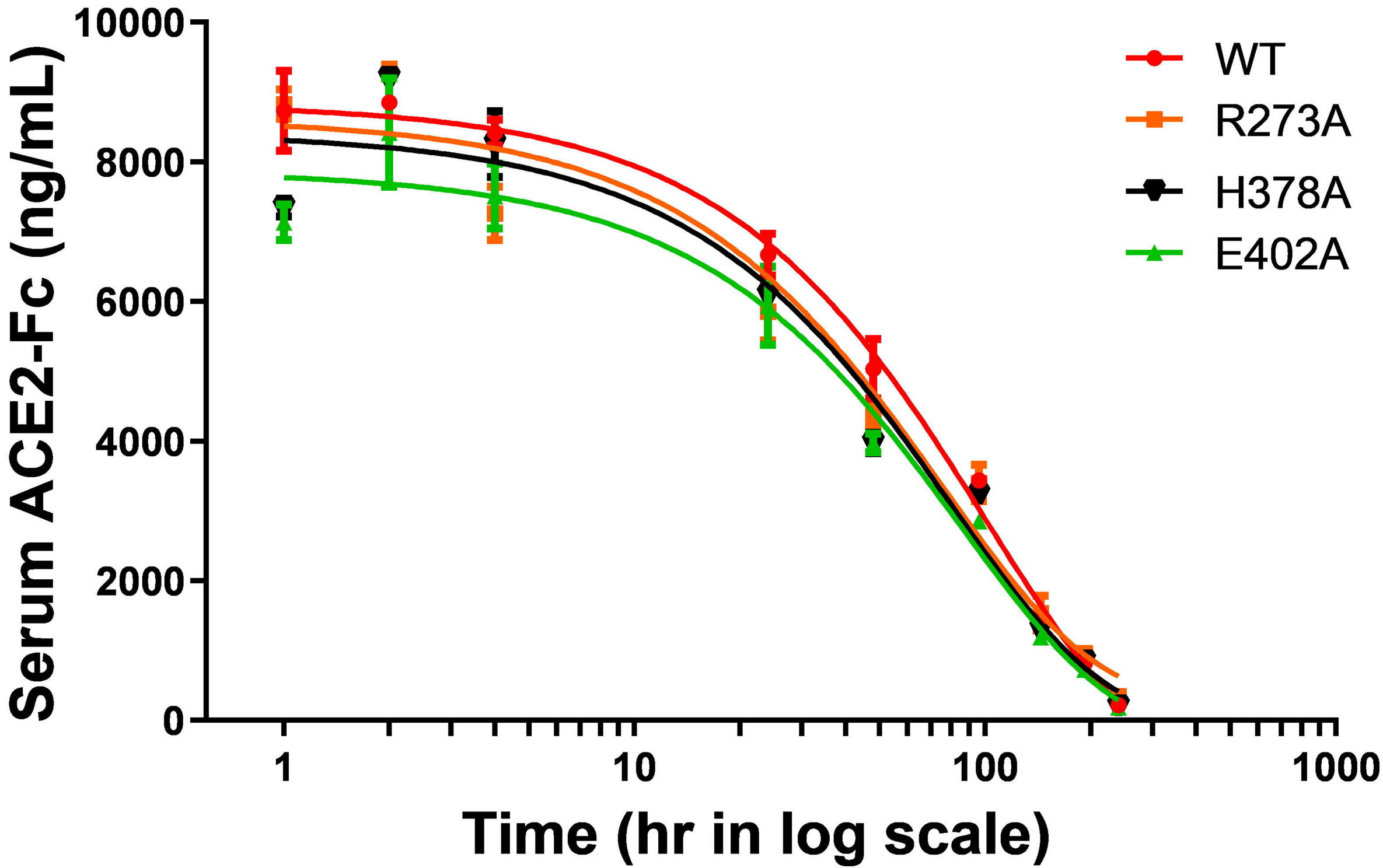
Serum ACE2-Fc (ng/mL)
10000
8000
6000
4000
2000
0
1
10
100
1000
Time (hr in log scale)
WT
R273A
H378A
E402A